



Design and Performance of the SOLAR-Induced Fluorescence Spectrometer of BISME

Yazhou Jing^(✉), Pengfei Duan, Bicen Li, and Weigang Wang

BISME, Beijing, China
15810106739@163.com

Abstract. At the end of 2020, the Chinese government proposed the goals of “carbon peaking and carbon neutrality”, which quickly became the focus of the times. The quantitative remote sensing needs of “carbon monitoring” are very urgent.

In the field of vegetation remote sensing, the solar-induced fluorescence remote sensing is a new type of remote sensing technology developed rapidly in recent years, and is the most breakthrough research frontier in the field of vegetation remote sensing in the past decade. Vegetation chlorophyll fluorescence has obvious advantages in photosynthesis detection, so it will play a very important role in vegetation monitoring and carbon cycle application.

This paper introduces the design scheme and performance of a spectrometer for the solar-induced fluorescence, including the task analysis, requirements, configurations and results of the instrument. This spectrometer was developed by the Beijing Institute of Space Mechanics and Electricity, and has been successfully launched in August 2022, entering the stage of in-orbit service.

Keywords: Carbon peaking and carbon neutrality · Solar-induced fluorescence remote sensing · Spectrometer · Design scheme and performance

1 Summary

Subsequent paragraphs, however, are indented. Vegetation fluorescence detection is to obtain the spatially continuous vegetation fluorescence signal by means of ultra high spectral resolution detection under the condition of weak reflection signal, analyze the photosynthesis capacity of land vegetation, and further answer and explain the carbon absorption capacity of forests and other vegetation and the growth of agricultural crops [1–4]. The task of the Sun Induced Fluorescence Spectrometer (hereinafter referred to as the Spectrometer) is to obtain the sun induced vegetation fluorescence remote sensing data, so as to accurately map the spatial and temporal distribution of regional/global vegetation fluorescence, and meet the needs of global carbon source, carbon sink quantitative monitoring, and forest vegetation productivity assessment [5–8].

This spectrometer was developed by Beijing Institute of Space Mechanics and Electricity, and has been successfully launched in August 2022, entering the orbit service phase.

2 Task Analysis

Photosynthesis of plants is the most basic biochemical process on the earth. Plants absorb carbon dioxide in the air, convert it into organic matter, and release generated oxygen into the air at the same time. Photosynthesis of green plants in terrestrial ecosystems is an important part of the earth's carbon absorption, and also an important way for the earth's ecosystem to achieve carbon neutralization [9, 10].

Chlorophyll fluorescence spectrum is narrow, only nanometer wide, and its energy is very weak in the reflected energy of vegetation, only about 0.5% to 2% of which is emitted in the form of fluorescence. Therefore, the spectrometer needs the detection ability of high spectral resolution, high signal to noise ratio and high stability [11, 12].

3 Indicator System

The design requirements of the hyperspectral detector should aim at the spectrum and radiation characteristics of chlorophyll fluorescence, combine the satellite orbital height and observation requirements, and comprehensively consider the spectral range, spectral resolution, spatial resolution, swath, signal-to-noise ratio and dynamic range of the detector. Through analysis and simulation, the indicator system of the spectrometer is shown in the following Table 1.

Table 1. The design Requirements of the spectrometer

Serial No	Project	Performance index requirements
1	Spectral range	670 nm–780 nm
2	spectral resolution	≤ 0.3 nm
3	Spectral sampling interval	≤ 0.15 nm
4	GSD	≤ 1.5 km
5	SNR	≥ 200 (input radiance 10 mWm ⁻² sr-nm-1)
6	Dynamic range of radiance	10– 350 mWm ⁻² sr-1nm-1
7	System MTF (static)	≥ 0.2 (Nyquist frequency)
8	width of cloth	≥ 30 km
9	Keystone/Smile Distortion	Less than 0.3 pixels
10	Stray light	$\leq 1\%$
11	Polarization sensitivity	$\leq 1\%$
12	Radiometric calibration accuracy	On board absolute radiometric calibration accuracy $\leq 5\%$
13	Spectral calibration accuracy	$\leq \Delta\lambda / 10$

4 Instrument Configurations

4.1 System Composition

The spectrometer consists of three single component, including optic-structure, signal processor and power unit. The system composition and functional block is shown in the following figure (Fig. 1).

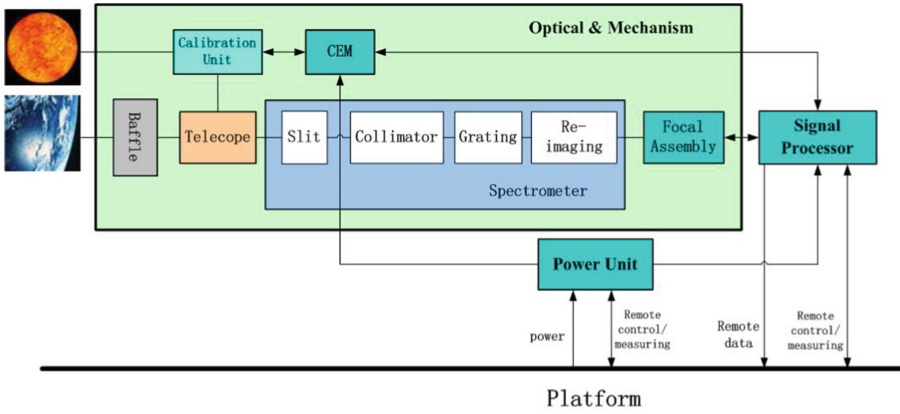


Fig. 1. Function and Composition Block of the spectrometer

4.2 Working Principle

The spectrometer adopts push scan imaging mode. The optical axis is perpendicular to the flight direction, the along orbit direction is the spectral dimension, and the through orbit direction is the spatial dimension. The input signal enters the spectrometer through the optical slit after passing through the telescope system. The transmitted collimation system expands the beam into parallel light and shines on the grating to disperse into fine spectrum. The spectrum is obtained by imaging on the focal plane detector through the convergence system. The analog signal of the focal plane detector is collected, amplified and converted into digital signal by A/D, and then processed and formatted. It is transmitted to the ground through the satellite data transmission system (Fig. 2).

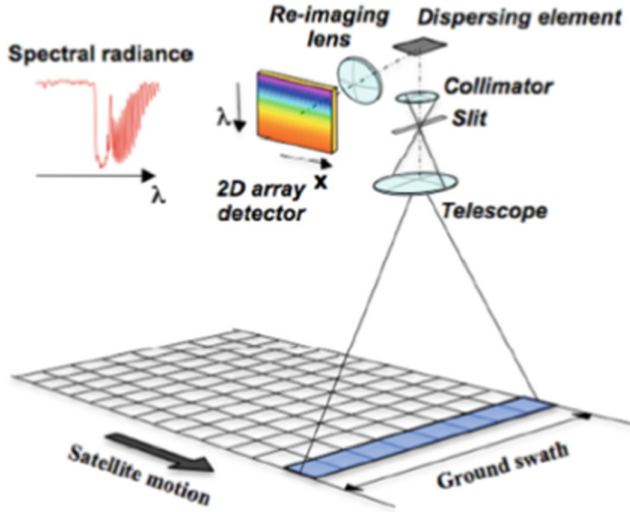


Fig. 2. Schematic diagram of the working principle of the spectrometer

4.3 Operating Mode

The spectrometer mainly has four working modes: launch mode, standby mode, observation mode and calibration mode, as shown in the following table (Table 2).

Table 2. Working Mode Design

Serial No	Project	Performance index requirements
1	Launch	To the orbit, power-off, mechanism locked
2	Standby	Waiting to work, thermal control, power-off
3	Activation	Observing, power-on
4	Calibration	Calibration on orbit: Solar calibration & Background calibration

The on orbit working mode of the spectrometer is shown in the figure below (Fig. 3).

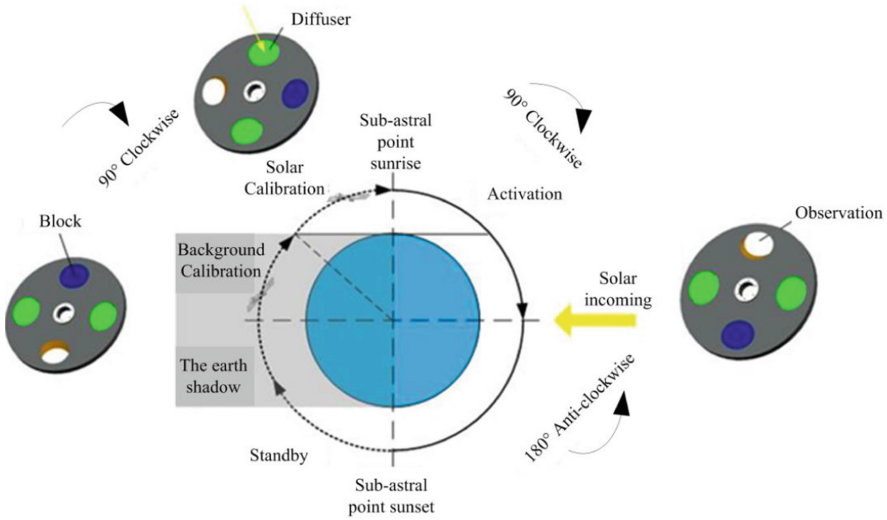


Fig. 3. On orbit operation mode of the spectrometer

4.4 Optical System Design

4.4.1 Optical System Composition

The order of the spectrometer optical path is as follows: radiation incident to the ground field of view or calibrated sunlight incident, then the energy enters the main optical and mechanical components, and finally converges on the detector. According to the function, the optical mechanical components can be divided into calibration components, telescope system components, spectrometer system components and focal plane components. The calibration components include calibration mechanisms and calibration controllers. The spectrometer system components include slit and field mirror components, collimation components, grating components and imaging components according to the detection order. As shown in the figure below (Fig. 4).

4.4.2 Optical System Design Results

In the optical system design of the spectrometer, in addition to the fine optical simulation, the influence of stray light and polarization on the imaging quality is fully considered. After establishing the simulation model of stray light, through multiple ray tracing, check the path of stray light, modify the structure that causes the stray light, and adopt the polarization suppression design of the double depolarizer, which ensures the detector's high-precision detection of weak target signals.

The comparison between the design results of the optical system of the spectrometer and the index system is shown in the following table (Table 3).

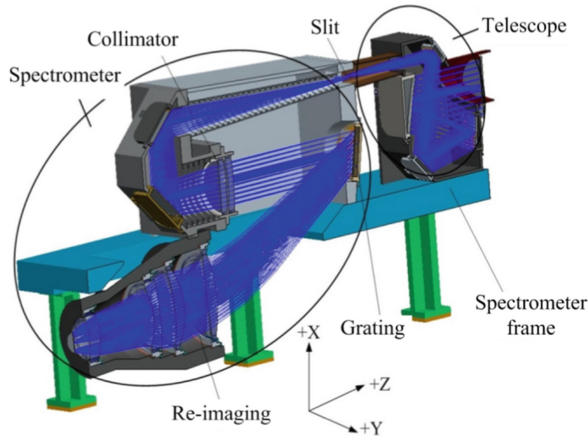


Fig. 4. Composition of main optical mechanical components

Table 3. Optical System Design Results

Indicator items	Index requirements	Design results
Working spectrum section	670 nm–780 nm	670 nm–780 nm
Spectral resolution	0.3 nm	0.3 nm
Spectral sampling interval	0.1 nm/pixel	0.1 nm/pixel
Spectral sampling rate	≥ 2.8 pixel ≤ 3.2 pixel	2.8 pixel–3.08 pixel
Focal length (rail crossing/space direction)	185 mm	185 mm
F	$2.7 \leq (F \text{ through} * F \text{ along}) / 2 \leq 2.8$	2.78
Field angle	$2\omega = 3.9^\circ$	3.9
Optical system transmissivity	≥ 0.65	0.7
MTF	$\geq 0.9 @ 1.85 \text{ lp/mm}$	0.98 @ 1.85 lp/mm
MTF	$\geq 0.9 @ 7.4 \text{ lp/mm}$	0.96 @ 7.4 lp/mm
Keystone	≤ 0.2 pixel	0.10 pixel
Smile	≤ 0.2 pixel	0.15 pixel

4.5 Optical Mechanical Structure Composition

The opto mechanical structure of the detector is composed of the base plate, calibration unit, optic-structure and thermal control unit. The detailed composition is shown in the table below (Table 4).

Table 4. Optical and Mechanical Structure Composition

Serial No	Components	
1	Base Plate	
2	Calibration Unit	Frame
3		Mechanism
4		Diffusers
5		Cover
6		Optic-structure
7	Optic-structure	Frame
8		Silt
9		Collimator
10		Grating
11		Re-imaging
12		Thermal Control
13	Focal plane heat-pipe	
14	Radiator	
15	LMI, heaters, etc	
16	Focal assembly	

4.6 Thermal Control Design

The spectrometer has high requirements for spectral resolution, stability and signal-to-noise ratio. The spectrometer system uses a plane reflective grating, which has high requirements for temperature gradient, temperature level and temperature stability. At the same time, the spectrometer is a high signal-to-noise ratio detector for weak signals, and reducing noise is one of the main means to improve the signal-to-noise ratio. Noise is mainly affected by device temperature noise and readout noise, so reducing device temperature is the main means to suppress device noise. The spectrometer operates in the sun synchronous orbit with an orbital period of about 90 min. Each circle has to go in and out of the earth's shadow, and the external heat flow conditions are complex, which makes the thermal control design of the spectrometer more difficult. Therefore, the spectrometer adopts the following thermal control measures.

- a. Integrated design of indirect thermal control and structure. The spectrometer has been optimized in structure, and a series of auxiliary structures have been added. By controlling the temperature of such auxiliary structures, a good thermal environment is provided for key components to form an indirect temperature control and meet the temperature stability requirements;
- b. Combination of passive thermal control and active thermal control, and use mature technologies as far as possible, such as thermal control coatings, multi-layer thermal

insulation materials, thermal insulation pads, thermal conductive fillers, film electric heaters and other measures;

- c. Compensated heating method is adopted to ensure the temperature stability of key components and reasonably allocate heating power.

4.7 On Orbit Calibration Scheme

The improvement of data accuracy depends on the high-precision radiometric calibration and spectral calibration of the instrument. In addition to providing complete instrument calibration parameters through laboratory calibration, accurate and reliable in orbit calibration is also required to eliminate the inconsistency between heaven and earth caused by space environment. The key to achieve high-precision calibration on orbit is to select appropriate calibration scheme and stable and reliable calibration source. The spectrometer uses the sun as the radiation calibration source, and achieves full aperture, full field of view, and full optical path absolute radiation calibration through the diffuser.

The on orbit calibration mode of the spectrometer includes solar calibration and circuit background calibration.

4.7.1 Solar Calibration Mode

The solar calibration shall be carried out at an appropriate time between the satellite's departure shadow area and the subsatellite point before the daytime. Turn the diffuser to the front of the main lens of the optic-structure, and the solar calibration lasts for about 36s. The solar calibration is performed once a day, and the primary diffuser and standby diffuser switching is performed once a month.

4.7.2 Circuit Background Calibration Mode

The circuit background calibration is carried out in the satellite shadow area. Turn the dark background block to the front of the main lens of the optic-structure, and the dark background calibration lasts for about 36s. The dark background calibration is conducted once a day.

5 System Verification

5.1 Validation Items

The spectrometer has been fully tested and verified in the laboratory. In order to ensure the validity and accuracy of the verification, all verification items are carried out under vacuum conditions. The verification items include radiometric calibration, spectral calibration, stray-light suppression test, polarization sensitivity test, BSDF test, etc. The test results provide a good data basis for the calibration and use of the spectrometer in orbit.

5.2 Validation Results

The laboratory test results of the spectrometer are summarized in the following table (Table 5).

Table 5. Test Results of the spectrometer

Indicator items	Requirements	Configurations	Compliance
Spectrum	670–780 nm	670–780 nm	C
Spectral Resolution	≤ 0.3 nm	0.3 nm	C
SSI	≤ 0.15 nm	0.1 nm	C
Swath	≥ 30 km	34 km	C
SSD	≤ 1.5 km	1.5 km	C
SNR	≥ 200	513.5	C
Radiation Calibration	absolute $\leq 5\%$	4.81%, on orbit	C
	relative $\leq 3\%$	2.2% in lab	C
Spectrum Calibration	$< 1/10 * \text{FWHM}$	$< 1/50 * \text{FWHM}$, on orbit & in lab	C

6 Conclusion

The spectrometer is a precision optical instrument for sun induced vegetation fluorescence detection. The system adopts the technical scheme of pushbroom imaging and grating dispersion light splitting. It has carried out comprehensive task analysis, fine system design and full test verification. All indicators meet and exceed the requirements of the detection task, and has the detection capabilities of high spectral resolution, high signal to noise ratio and high stability. After being officially put into operation, the spectrometer will play a very important role in vegetation monitoring and carbon cycle applications [13, 14].

References

1. Sun, Y., et al.: OCO-2 advances photosynthesis observation from space via solar-induced chlorophyll fluorescence. *Science* **358**(6360), eaam5747 (2017)
2. Frankenberg, C. et al.: New global observations of the terrestrial carbon cycle from GOSAT: patterns of plant fluorescence with gross primary productivity. *Geophys. Res. Lett.* **38**(17) (2011)
3. Damm, A., et al.: Far-red sun-induced chlorophyll fluorescence shows ecosystem-specific relationships to gross primary production: an assessment based on observational and modeling approaches. *Remote Sens. Environ.* **166**, 91–105 (2015)
4. Joiner, J., et al.: Global monitoring of terrestrial chlorophyll fluorescence from moderate-spectral-resolution near-infrared satellite measurements: methodology, simulations, and application to GOME-2. *Atmos. Measur. Tech.* **6**(10), 2803–2823 (2013)
5. Du, S., et al.: Retrieval of global terrestrial solar-induced chlorophyll fluorescence from TanSat satellite. *Sci. Bull.* **63**(22), 1502–1512 (2018)
6. Coppo, P., Taiti, A., Pettinato, L., Francois, M., Taccola, M., Drusch, M.: Fluorescence imaging spectrometer (FLORIS) for ESA FLEX mission. *Remote Sens.* **9**(7), 649 (2017)
7. Drusch, M., et al.: The fluorescence explorer mission concept-ESA's earth explorer 8. *IEEE Trans. Geosci. Remote Sens.* **55**, 1273–1284 (2016)

8. Guanter, L., et al.: Developments for vegetation fluorescence retrieval from spaceborne high-resolution spectrometry in the O2-A and O2-B absorption bands. *J. Geophys. Res.* **115**(D19) (2010)
9. Ma, Y., Liu, L., Chen, R., et al.: Generation of a global spatially continuous TanSat solar-induced chlorophyll fluorescence product by considering the impact of the solar radiation intensity. *Remote Sens.* **12**(13), 2167 (2020)
10. Coppo, P., Pettinato, L., Nuzzi, D., et al.: Instrument predevelopment activities for FLEX mission. *Opt. Eng.* **58**(7), 075102 (2019)
11. Abdon, S., et al.: Digital correction of residual straylight in FLEX images. In: *SPIE Proceedings of the International Conference Space Optics ICSO*, Chania, Greece (2018)
12. Taiti, A., Coppo, P., Battistelli, E.: Fluorescence imaging spectrometer optical design. *Proc. SPIE* **9626**, 96261N (2015)
13. Meroni, M., et al.: Remote sensing of solar-induced chlorophyll fluorescence: review of methods and applications. *Remote Sens. Environ.* **113**, 2037–2051 (2009)
14. Du, S., Liu, X., Chen, J., Liu, L.: Prospects for Solar-induced chlorophyll fluorescence remote sensing from the SIFIS Onboard the TECIS-1 satellite. *J. Remote Sens.* 2022, Article ID 9845432, 9 pages (2022)